

PAPER

Resourcefulness, robustness, and recovery: tail use during climbing in rats

Brian M. Woronowicz,^{1,2,*} Noah C. Graber,¹ Shahin G. Lashkari^{1,2}
and Noah J. Cowan^{1,2}

¹Mechanical Engineering Department, Johns Hopkins University, 3400 North Charles Street, 21218, Maryland, USA and ²Laboratory for Computational Sensing and Robotics, Johns Hopkins University, 3400 North Charles Street, 21218, Maryland, USA

*Corresponding author. bworono1@jhu.edu

FOR PUBLISHER ONLY Received on Date Month Year; revised on Date Month Year; accepted on Date Month Year

Abstract

Tails serve diverse evolutionary functions across species, but their mechanical role during complex climbing maneuvers remains understudied. We investigated how Long-Evans rats (*Rattus norvegicus*) use their tails when climbing up and over a ledge with a climbing bar positioned 23–32cm above a bottom platform. Using force measurements and motion tracking, we quantified tail-generated impulse during climbing and found that tail usage followed an inverse relationship between the impulse they imparted to the bottom platform and the usage of their tail: a higher initial jumping impulse required less assistance from the tail, while a lower initial momentum required a greater compensatory force from the tail. When climbing from greater depths (up to 32cm), rats maintained consistent jumping impulse but significantly increased tail usage, suggesting a preference for a reliable strategy with mid-climb adjustments rather than pre-calibrated jumping force. Rats demonstrated one-shot learning when the forelimb torque was eliminated by covertly unlocking the climbing bar. After a single near-failure, they shifted from a dynamic, ballistic climbing style to a more controlled, quasistatic approach. This new method involved increased tail usage and adjusted body positioning to reduce gravitational moments. These findings reveal that rats employ their tails as actively controlled limbs that contribute substantial forces during complex maneuvers, adapting usage based on initial conditions and mechanical constraints.

Key words: climbing, tail, rats, biomechanics, template model, jumping

1 Introduction

Tails serve critical mechanical roles in locomotion (Hickman, 1979), particularly during challenging maneuvers like climbing (Jusufi et al., 2008; Lacava et al., 2024; Shield et al., 2021) and aerial self-righting (Bartholomew and Caswell, 1951; Libby et al., 2012; Schwaner et al., 2021) where tails provide stability, force generation, and rapid, dynamic adjustments to unexpected perturbations. Here, we focus on tail use during climbing which provides a particularly informative context for studying how tails are deployed to actively interact with the environment, for example to counteract pitching moments (Norberg, 1986; Siddall et al., 2021) and even arrest falls when feet lose purchase (Jusufi et al., 2008).

Recent advances have highlighted the tail's role in both biological and artificial climbing systems. In mice, tails play an integral role in rotational control and balance correction during rapid maneuvers (Lacava et al., 2024). Robotic systems have incorporated biologically inspired tails under both feedforward (Buckley et al., 2023) and feedback (Jusufi et al., 2008) control to improve climbing stability on uncertain terrain. Together, these developments suggest that the tail is not simply a passive

stabilizer, but an adaptable effector with real-time feedback control potential.

Rats (*Rattus norvegicus*) provide an ideal model for investigating tail function in climbing due to their combination of physical adaptability and cognitive capabilities. Their intelligence enables reliable performance of trained behaviors, while their natural locomotor abilities make them excellent subjects for studying climbing (Makowska and Weary, 2016; Notomi et al., 2001). However, the role of their tails during climbing maneuvers remains largely unexplored.

To take the next step, we developed a behavioral paradigm in which a rat leaps out of a ditch and onto a ledge equipped with a “pull-up bar”; see Figure 1 and Supplemental Video S1. We examined the mechanical demands of this climbing behavior through principles of angular momentum balance applied to a simplified template model (Full and Koditschek, 1999) (Figure 1). When climbing up and over the ledge, the rat must generate sufficient angular impulse about the pull-up bar to overcome gravitational moments, which serve to deplete angular momentum. We consider three possible sources of this compensatory angular impulse: the initial vertical impulse at take-off, angular moments provided by the forelimbs on the

pull-up bar, and angular moments provided by the tail on the tail platform.

In the template model, it is assumed that the rat leaps vertically with an initial vertical leaping impulse of P_b , with an offset horizontally relative to the pull-up bar of L_g . This generates an initial angular impulse about the pull-up bar of

$$\text{Angular impulse @ take-off} = L_g P_b. \quad (1)$$

Once airborne, the center of mass of the rat travels vertically, and gravity begins to deplete the angular momentum, namely

$$\text{Angular momentum during flight} = L_g P_b - L_g m g t, \quad (2)$$

where t is measured from the beginning of take-off. Once the animal grips the pull-up bar, we assume a simplified rigid body, with constant moment of inertia I about the pull-up bar, undergoing angular motion with instantaneous angular velocity ω . (As real rats climb, their bodies do in fact bend and change shape, impacting, for example, the angular moment of inertia, but our simplified model neglects this.) Computing angular momentum balance about the attachment point gives rise to the following simplified dynamics:

$$I\dot{\omega} = F_t L_t - m g L_g + \tau_f u_{lock}, \quad (3)$$

where $\dot{\omega}$ is the angular acceleration, F_t is the force applied by the tail, L_t is the moment arm of the tail force, m is the mass of the rat, g is gravitational acceleration, L_g is the horizontal distance from the center of mass to the attachment point (which will change as the body rotates around the bar), τ_f is the torque applied by the forelimbs on the attachment point, and u_{lock} is a binary variable equal to 1 when forelimbs can produce a torque at the attachment point and 0 when they cannot. This binary variable captures a key component of our test platform design, namely that the pull-up bar can be “unlocked” such that it spins freely, eliminating torques that the forelimbs can otherwise provide in the “locked” condition.

This template model motivated specific, mechanistic predictions: (i) tail force should inversely correlate with initial jumping impulse; (ii) at larger climbing depths, animals should compensate by increasing their initial impulse, their tail-generated force, or both; and (iii) eliminating the animals’ forelimb-generated moments should result in greater tail-generated moments, shortened gravitational moment arms, or both. In this study, we tested these predictions using a custom experimental setup that quantifies take-off and tail forces in *R. norvegicus* climbing up and over a ledge in mechanically stable (“locked”) and unstable (“unlocked”) conditions.

Materials and Methods

Animals and Training

Five adult male Long Evans rats (*Rattus norvegicus*) were obtained from Inotiv for this study. Animals were individually housed in cages with running wheels. Previous work has shown that rodents raised in a generic lab housing environment perform poorly in balance tasks even with intact tails, suggesting that tail-based motor skills need to be learned through experience (Buck et al., 1925). Therefore, we trained the animals in large wire enrichment cages equipped with elevated platforms and connecting ramps where animals could develop their motor skills and confidence while climbing.

Animals could begin training on the actual experimental rig after demonstrating the ability to navigate the cage environment skillfully, including climbing the wire sides, jumping between platforms, and accessing elevated platforms without using the provided ramps. Rats were individually housed on a 12/12-h light/dark cycle, and all training and experiments were conducted during the dark portion of the cycle. The rats were 5–12 months old and weighed 325–400 g at the time of the experiments. All animal care and housing procedures complied with National Institutes of Health guidelines and followed protocols approved by the Institutional Animal Care and Use Committee at Johns Hopkins University.

Experimental Apparatus

Rats were trained to climb up onto a ledge from a bottom platform with variable depth ranging from 23 to 32 cm. A 0.64 cm diameter “pull-up bar,” highlighted in orange in Figure 1A-C, was placed at the ledge and wrapped in waterproof anti-slip tape. A set screw could be used to lock the bar, allowing for forelimb-generated moments (example trial in Supplemental Video S1), or unlock the bar, allowing it to freely spin, eliminating forelimb-generated moments (example trial in Supplemental Video S2). The bottom platform (pink) and ledge (blue) were instrumented with single-axis load cells (HBK PW6D Single Point Load Cell, model 1-PW6DC3/5KG-1) to quantify the vertical ground-reaction forces at takeoff from the bottom and “pull-up” forces on the ledge, respectively. A third force plate (green) was positioned 10 cm away from the pull-up bar and at a 30° offset from the ledge, allowing the animal to push off with its tail. This configuration ensured that the normal forces recorded by the tail platform load cell were the forces directly providing moments to the animals’ centers of mass about the pull-up bar (Figure 1C). When calculating tail moments, we used the most conservative estimate by taking the shortest distance from the tail platform to the pull-up bar as the moment arm, since the exact center of pressure of the distributed tail load could not be determined.

The sessions were filmed using a FLIR Blackfly S camera with a custom adaptive frame rate. The camera recorded at 20 frames per second during periods of no force plate activity and automatically increased to 200 frames per second when forces were detected on any platform. All force data was collected at 2000 Hz through a National Instruments data acquisition system controlled by LabVIEW software. This adaptive frame rate allowed us to capture high-speed movements during climbing without taking up excessive hard drive space during periods of inactivity.

Experimental Protocol

We designed our experiment to investigate the role of tail dynamics during vertical climbing maneuvers under varied conditions. Trials were defined as one iteration of an animal climbing from the bottom platform to the top of the ledge. A successful trial needed to meet specific criteria: during the climbing motion, the hindlimbs of the animals were not permitted to make contact with the tail platform. This ensured that forces recorded on the tail platform were exclusively from tail interactions. **Trials where hindlimbs made contact with the tail platform were detected via manual inspection and not included in analysis.**

Trials were conducted in two types of sessions: locked bar sessions and variable bar sessions. During locked bar sessions, the pull-up bar remained static for the duration of each session.

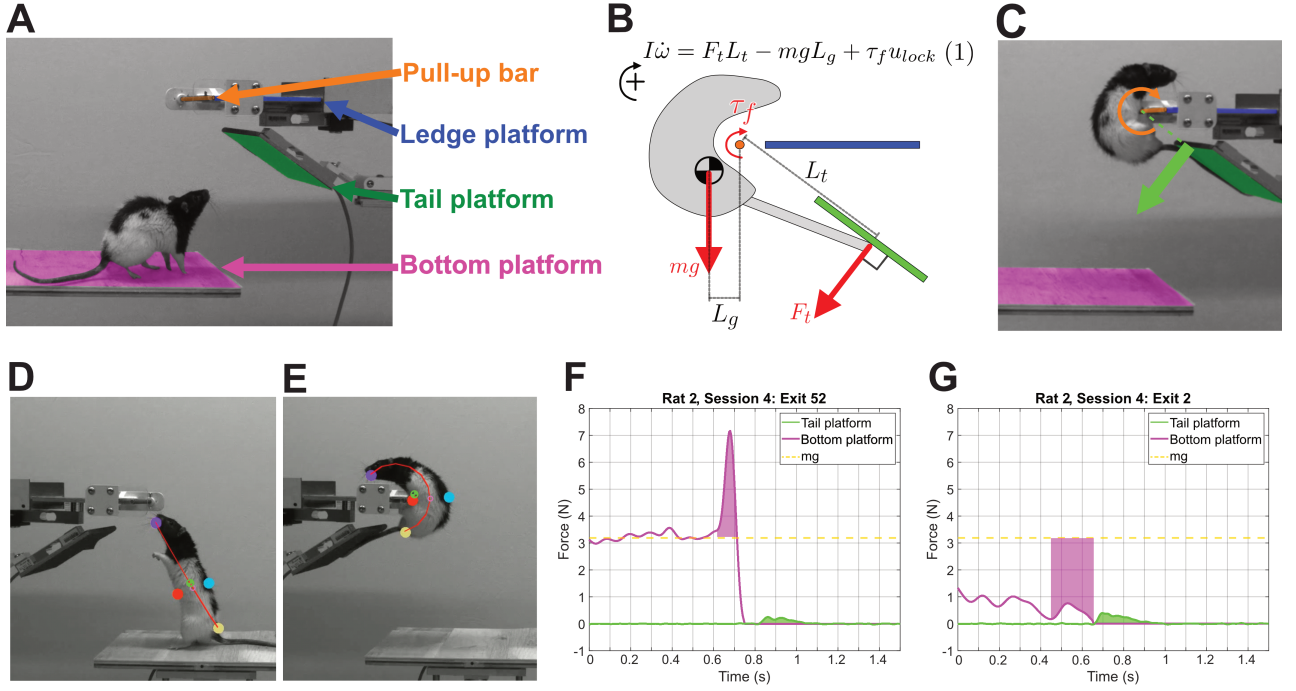


Fig. 1. (A) Experimental apparatus showing the bottom platform (magenta), ledge platform (blue), tail platform (green), and pull-up bar (orange). (B) Template model schematic illustrating the moments about the pull-up bar during climbing. (C) Example of tail moment arm estimation. (D, E) DeepLabCut tracking points showing body posture during extended (D) and curved (E) configurations. (F, G) Example force traces during exits: bottom platform force in magenta, tail platform force in green, and body weight in yellow. (F) shows an exit with a positive bottom platform impulse, and (G) shows an exit with a negative bottom platform impulse.

In variable bar sessions, the bar state was changed (e.g., locked to unlocked). Locked bar sessions typically lasted 30 minutes. In variable bar sessions, since we would switch the bar state after a minimum of 25 minutes of baseline data collection, these sessions ranged from 45-60 minutes.

Additionally, we examined the effects of bottom platform depth on vertical climbing maneuvers. Locked bar sessions were conducted at different depths. Platform depth was static throughout the duration of each session. Sessions ranged in bottom platform depth from 23 to 32 cm (where the maximum depth for each animal was the depth where they could successfully complete trials in the intended manner).

Motion Tracking and Modeling

Animal movements were tracked using DeepLabCut (Mathis et al., 2018), a markerless tracking program that identified four key anatomical landmarks (Fig. 1D-E): mouth (purple), tail base (yellow), belly (red), and mid-spine (cyan). These tracking points were used to estimate the animal's center of mass (CoM) through a geometric approach that is similar to methods used in squirrel locomotion literature (Hunt et al., 2021; Lee et al., 2025). Each video frame contained a circle segment (red) that started at the mouth, passed through the midpoint between the mid-spine and belly markers, and ended at the base of the tail. These markers were selected to ensure the fitted circle segment would closely approximate the animal's body centerline in both extended (Fig. 1D) and highly curved (Fig. 1E) postures. This circle was divided into ten segments, each with a unique weight. The center of mass was then computed as the weighted average of these segments, providing an estimate of the animal's mass distribution throughout the climbing motion. The weights of

the segments were chosen so that the estimated center of mass fit measurements of centers of mass obtained from rat cadaver studies. Each generated center-of-mass trajectory was manually inspected to ensure tracking accuracy. While the DeepLabCut models were generally robust across a wide range of postures, occasional tracking errors were identified and filtered out prior to analysis.

To interpret the moments acting about the pull-up bar, we developed a highly simplified template model (Full and Koditschek, 1999) in the sagittal plane. The model comprises a two-dimensional rigid body that pivots about the pull-up bar as shown in Figure 1B. The momentum balance about the pull-up bar is governed by the relationship established in Equation 3 in the introduction, where the moment of inertia I , angular acceleration $\dot{\omega}$, tail force F_t , moment arms L_t and L_g , and forelimb torque capabilities are the key parameters determining climbing dynamics.

Using the tracked center-of-mass position, we could calculate L_g for each frame, while L_t was taken to be the shortest distance from the pull-up bar to the tail platform.

Data Processing

For each identified climbing event, impulse were calculated from the force data through a multi-step process. First, the animal's weight (measured prior to each session) was subtracted from the raw force readings to isolate the dynamic forces associated with climbing; thus, positive bottom platform impulse indicate forces exceeding body weight, while negative bottom platform impulse indicate forces less than body weight. Negative bottom platform impulse typically occurred when animals initiated weight transfer to the pull-up bar before completing their climb,

resulting in reduced forces on the bottom platform. Because body weight is not subtracted from the tail platform force reading, tail impulse are always positive. The temporal bounds of each impulse were determined by identifying the last force peak before the platform reading returned to its unloaded baseline. Impulse values were then calculated by integrating the weight-corrected force data between these bounds. A similar process was applied to tail platform data, with the additional criterion that only force applications verified to be from the tail (and not hindlimb contact) were included in the analysis.

Statistics

Statistical analysis was performed using MATLAB R2024a (MathWorks). Linear relationships between force impulse were assessed using MATLAB's `fitlm` function to create linear regression models. For outlier detection, Cook's distance was calculated for each observation using MATLAB's diagnostics tools. Data points with Cook's distance values exceeding three times the mean Cook's distance were identified as outliers and removed from the dataset. After outlier removal, we recomputed the linear regression on the cleaned dataset to obtain the final model parameters. Statistical significance of the linear relationships was assessed by examining the p-values of the slope coefficients, with significance determined at $\alpha = 0.05$. R^2 values and p-values are reported for all regression analyses. For comparisons between distributions, the Wilcoxon ranksum test was employed. This non-parametric approach was chosen as it does not require the assumption of normally distributed data. For these tests, p-values are reported. All data are presented as mean \pm standard deviation unless otherwise specified.

To examine how task conditions affected trial-level impulse data while accounting for repeated measures, we used linear mixed-effects models (LMMs) implemented via MATLAB's `fitlme` function. Models included rat identity as a random effect, and in some cases session identity nested within rat (`(1|RatID:SessionNum)`) to account for hierarchical structure in the dataset. Fixed effects varied by analysis and included bottom platform impulse, pull-up bar condition (locked vs. unlocked), ditch depth, trial number, and animal weight. Outliers were removed using a z-score threshold of ± 3 standard deviations (via MATLAB's `isoutlier(..., "mean")`), applied separately to tail and bottom impulse distributions. After tuning, final models were used to test the statistical significance of fixed effects, with $\alpha = 0.05$.

Results

Increases in Bottom Platform Impulse Reduced Reliance on Tail Use

As rats increased their bottom platform jumping impulse, they relied less on tail platform impulse; see Figure. 2. A significant inverse relationship between tail and bottom platform impulse was robust across all five animals during locked-bar sessions. For Rat 1, only one session was recorded, and it showed this statistical negative correlation. The statistically significant negative correlation was found in 3 out of 4 sessions for rat 2, 2 of 6 for rat 3, 1 of 6 for rat 4, and 4 of 5 for rat 5. No session in any animal exhibited a statistically significant positive correlation. The consistency of this relationship across multiple animals and sessions suggests a behavioral pattern in the climbing strategy.

To assess the robustness of this pattern, we conducted a binomial test to determine whether the observed number of significant results—11 out of 22 sessions—could plausibly occur by chance. Under the null hypothesis that each session has a 5% chance of being significant due to random variation ($\alpha = 0.05$), we would expect approximately $0.05 \times 22 = 1.1$ significant sessions by chance alone. The probability of observing 11 or more significant results under this null is given by the binomial expression $P(X \geq 11 | n = 22, p = .05) \ll .001$, strongly rejecting the null hypothesis. Additionally, we had an a priori hypothesis (based on pilot data) that the correlations would be negative, justifying one-tailed tests. All 11 significant effects were indeed negative, with none positive. Under the null hypothesis of a 50% chance for either direction, the probability of observing 11 out of 11 significant results in the same direction is $P = 0.5^{11} < .001$, further strengthening the case that this is a true and consistent effect.

To further confirm this relationship at the population level while accounting for inter-animal variability and repeated measures, we constructed an LMM predicting tail impulse from bottom platform impulse, ditch depth, trial number, and weight, with rat identity and session nested within rat included as random effects. The model revealed a significant negative effect of bottom platform impulse on tail impulse ($\beta = -0.0129 \pm 0.0020(\text{N}\cdot\text{s}/\text{N}\cdot\text{s})$, $p < .001$), consistent with the inverse relationship observed across individual sessions. By contrast, tail impulse increased significantly with ditch depth ($\beta = 0.0079 \pm 0.0014(\text{N}\cdot\text{s}/\text{cm})$, $p < .001$). Tail impulse also increased with trial number ($\beta = 0.00018 \pm 0.00002(\text{N}\cdot\text{s}/\text{trial})$, $p < .001$), suggesting possible adaptation, learning effects, and other order-dependent effects, though likely not fatigue (see bottom impulse results in the next section). Animal weight was not a significant predictor ($p = .43$). To give some intuition for the effects predicted by this model, a 1 cm increase in ditch depth led to an average increase in tail impulse of $0.0079\text{N}\cdot\text{s}$. In comparison, across a typical session with approximately 30 trials, the cumulative effect of trial number amounted to only $0.0054\text{N}\cdot\text{s}$ —about 68% the size of the ditch depth effect. The model accounted for variability at both the rat and session levels, with random effects capturing differences in baseline tail impulse across rats ($\text{SD} = 0.0180$) and sessions ($\text{SD} = 0.0107$).

This finding is consistent with Eq. 3 that predicts that as bottom platform impulse increase, the animal's initial vertical momentum becomes increasingly sufficient to complete the climbing motion, requiring proportionally less tail assistance. Conversely, as bottom platform impulse decrease, the animal must rely increasingly on tail-generated moments to supplement the climbing motion, likely in combination with forelimb forces at the pull-up bar.

As Bottom Platform Depth Increased, Rats Increased Tail Usage, Not Jump Impulse

We investigated how these impulse changed when navigating different depths. While we initially expected rats to modify both bottom and tail platform impulse when climbing to greater depths, we found that most animals selectively altered tail usage without changing bottom platform impulse.

As shown in Figure 3A, Rat 2's bottom platform impulse remained consistent between shallow (23 cm) and deep (26 cm) conditions (Wilcoxon rank-sum test, $p = .963$). In contrast, tail platform impulse increased significantly in the deeper condition (Wilcoxon rank-sum test, $p < .001$). This pattern was statistically significant in three of the four rats tested,

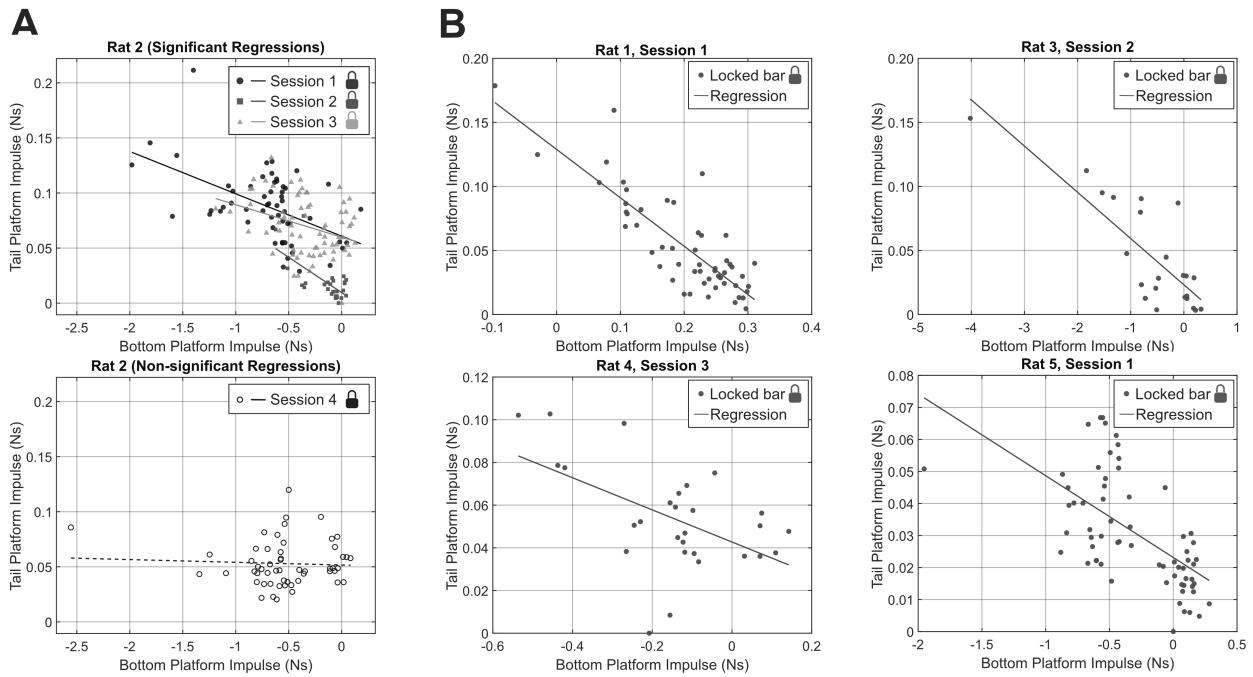


Fig. 2. Rats demonstrate a negative correlation between tail impulse and bottom platform impulse during locked bar sessions. **A.** Data from Rat 2 across all locked bar recording sessions, separated into significant (upper panel) and non-significant (lower panel) linear regressions. The panels show the relationship between tail impulse (*y*-axis) and bottom platform impulse (*x*-axis). Filled circles with solid regression lines indicate statistically significant correlations (upper panel: darkest gray: $n = 57$, slope = -0.0384 , $R^2 = 0.2656$, $p < .001$; medium-dark gray: $n = 28$, slope = -0.0641 , $R^2 = 0.4191$, $p < .001$; medium-light gray: $n = 70$, slope = -0.0295 , $R^2 = 0.1171$, $p = .004$), while unfilled circles with dashed regression lines indicate non-significant correlations (lower panel: $n = 54$, slope = -0.0025 , $R^2 = 0.0027$, $p = .708$). **B.** Representative data from the remaining 4 rats from this study during locked bar sessions, all showing statistically significant negative correlations between tail impulse and bottom platform impulse: Rat 1 ($n = 53$, slope = -0.378 , $R^2 = 0.703$, $p < .001$), with Rat 3 ($n = 23$, slope = -0.036 , $R^2 = 0.6754$, $p < .001$), Rat 4 ($n = 28$, slope = -0.075 , $R^2 = 0.282$, $p = .0037$), and Rat 5 ($n = 66$, slope = -0.026 , $R^2 = 0.3596$, $p < .001$).

demonstrating that these three animals adjusted their strategy during their climbing traversals rather than modifying their initial jumping forces. While only Rat 2's data are shown here, the corresponding plots for the other two rats exhibiting this pattern (Rats 3 and 5) can be generated using the provided data and plotting code.

Rat 4 displayed a notably different behavioral pattern (Figure 3B). Unlike the other animals, showing significant differences in both bottom and tail platform impulse between depth conditions ($p < .001$ for both comparisons). Quite surprisingly, bottom platform impulse became more negative in the deep condition despite the greater depth, while tail impulse increased significantly. Interestingly, this combination of decreased bottom platform impulse and increased tail impulse resembles strategies more commonly observed during unlocked bar conditions, which we examine in the next section.

To assess whether this pattern held across the population and ditch depths, while accounting for variability across rats and sessions, we fit an LMM predicting bottom platform impulse from ditch depth, trial number, and weight, with random effects for rat and session. Consistent with the per-animal analyses, ditch depth was not a significant predictor of bottom impulse ($\beta = -0.00094 \pm 0.0274$ (N·s/cm), $p = .97$), indicating that animals did not systematically alter their initial push-off forces when climbing from greater depths. Weight had a weak but statistically significant negative effect ($\beta = -0.0065 \pm 0.0030$ (N·s/g), $p = .027$), while trial number had a modest significant positive effect on bottom impulse ($\beta =$

0.00187 ± 0.00036 (N·s/trial), $p < .001$). The model accounted for session-level variation (random effect SD = 0.23). Together, these findings confirm that rats primarily adjusted tail usage, rather than jump force, to accommodate changes in platform depth.

Rats Rapidly Adapted Their Climbing Strategy after Forelimb Torque was Eliminated

The transition from locked to unlocked pull-up bar conditions resulted in immediate behavioral adaptation. As shown in Figure 4A, impulse from a representative Rat 1 session followed a significant negative regression during locked trials but showed no significant trend after the bar was unlocked, indicating a shift in climbing strategy.

During the first unlocked trial (marked with a black star in Figure 4A-B), the animal attempted to climb using its typical locked-bar strategy but lost forelimb footing under the freely spinning bar and needed to adapt mid-climb (Supplemental Video S3). This adaptation occurred in one-shot, as evidenced by the abrupt change in bottom platform impulse values in subsequent unlocked trials (Figure 4B).

This behavioral change was both rapid and significant across both impulse types. Bottom platform impulse decreased significantly in the unlocked condition ($p < .001$; Figure 4C), while tail platform impulse increased significantly ($p < .001$; Figure 4C). This pattern of adaptation was consistent across 4 out of 5 animals tested, showing significant decreases in bottom platform impulse ($p < .05$) and increases in tail platform

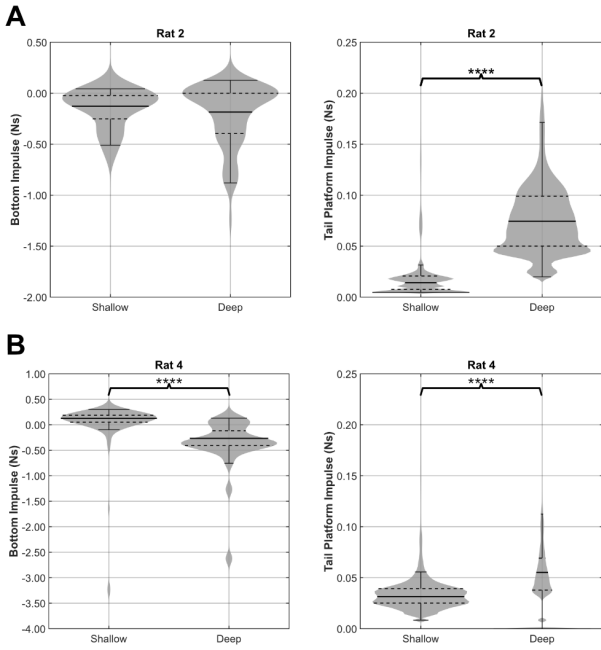


Fig. 3. Rats increased tail platform usage, not bottom platform impulse, when climbing from greater depths. **A.** Distribution of bottom platform impulse (left) and tail platform impulse (right) for Rat 2 under shallow (23 cm, $n = 28$) and deep (26 cm, $n = 76$) conditions. Bottom platform impulse remained consistent between depth conditions (Wilcoxon rank-sum test, $p = .755$), with the shallow condition averaging -0.127 ± 0.164 Ns and the deep condition averaging -0.185 ± 0.283 Ns. Tail impulse increased significantly in the deep condition (Wilcoxon rank-sum test, $p < .001$, marked with asterisks), with the shallow condition averaging 0.014 ± 0.007 Ns and the deep condition averaging 0.074 ± 0.031 Ns. Solid black lines indicate means, dashed lines represent quartiles, and whiskers represent the extrema of data, outside of which lies outliers. This pattern was representative of three of the four animals tested, showing strategic adaptation through increased tail usage rather than modified jumping force. **B.** Distribution of bottom and tail impulse for Rat 4, which displayed an atypical response pattern. Unlike the other animals, Rat 4 showed significant differences in both bottom platform impulse (left, shallow: 0.125 ± 0.095 Ns, $n = 87$; deep: -0.265 ± 0.229 Ns, $n = 30$; Wilcoxon rank-sum test, $p < .001$, marked with asterisks) and tail impulse (right, shallow: 0.032 ± 0.010 Ns; deep: 0.055 ± 0.026 Ns; Wilcoxon rank-sum test, $p < .001$, marked with asterisks) between depth conditions.

impulse ($p < .05$) in the unlocked condition. Rat 5 was the exception, also displaying a significant increase in tail impulse but the corresponding decrease in bottom platform impulse following the transition to the unlocked bar condition was statistically significant.

To assess the robustness of this pattern across animals, we fit LLMs predicting trial-level impulse from pull-up bar condition (locked vs. unlocked) and trial number, with rat identity as a random effect. Tail impulse increased significantly in the unlocked condition ($\beta = 0.0732 \pm 0.0090$ (N·s/N·s), $p < .001$). Trial number was not a significant predictor ($p = .67$). In contrast, bottom platform impulse significantly decreased in the unlocked condition ($\beta = -1.3525 \pm 0.137$ (N·s/N·s), $p < .001$), and showed a weak increase as a function of trial number ($\beta = 0.0043 \pm 0.0020$ (N·s/trial), $p = .03$). These findings confirm that the shift in climbing strategy following bar unlocking was both rapid and consistent across animals. The model also accounted for baseline differences in

bottom impulse across animals (random intercept SD = 0.38), indicating consistent effects despite individual variation.

Center-of-mass trajectories revealed distinct movement patterns between conditions (Figure 4D). In the locked condition, trajectories exhibited near-parabolic paths characteristic of ballistic motion, while unlocked condition trajectories showed an initial downward movement followed by an upward sweep to complete the climb. These trajectory differences align with the measured impulse changes, indicating that the animals developed a fundamentally different climbing strategy when forelimb torque was eliminated.

The relationship between peak gravity moment and peak tail moment across all rats (Figure 4E) further confirms this adaptive strategy, with animals generating higher tail moments in the unlocked condition to compensate for the increased gravitational challenges during climbing. In Figure 4F, it can also be seen that the average peak moments shift up to the “ $y = x$ ” line, indicating that, on average, the moments provided by the tail are matching the counteractive peak moments due to gravity on the center of mass.

In fact, all animals significantly adapted their moments to the spinning bar, though with varying strategies. Figure 4F shows the distributions of peak center-of-mass and peak tail moments of Rat 1 before and after unlocking the bar. Analysis reveals that this animal significantly decreased its peak magnitudes of its center-of-mass moments ($p < .001$) while simultaneously increasing its peak tail-induced moments ($p < .001$). This is 1 of 2 animals that adapted in this way. Another 2 rats adapted by keeping their peak center-of-mass moments the same and increasing their peak tail moments, while the remaining rat kept its tail moments the same and decreased its center-of-mass moments.

Discussion

Our results demonstrate that rats employ their tails as versatile, dynamically controlled tools during climbing, adapting usage based on both initial conditions and task demands. The observed inverse relationship between bottom platform impulse and tail usage, consistent bottom platform impulse with increased tail usage at greater depths, and rapid adaptation to mechanical changes reveal sophisticated motor control strategies. These findings extend our understanding of tail function beyond passive stabilization, showing that rats use their tails as actively controlled “fifth limbs” that contribute substantial forces during complex climbing maneuvers.

Relationship Between Bottom and Tail impulse

The strong negative correlation between bottom platform impulse and tail platform impulse demonstrates that rats dynamically modulate tail usage based on their initial momentum. This relationship makes mechanical sense when considered through the lens of angular momentum about the pull-up bar. When a rat generates higher initial vertical impulse from the bottom platform at a center-of-pressure that is offset from the pull-up bar, it induces a larger initial angular impulse (Eq. (1)). Once airborne, gravity begins to deplete this angular momentum (Eq. (2)). When the forelimbs grip the bar, angular momentum is conserved around the bar, and the rotation about the bar is governed by Eq. (3), according to this idealization. With sufficient initial angular momentum, the rat can successfully reach the top of the platform with minimal tail assistance. Conversely, when initial angular momentum

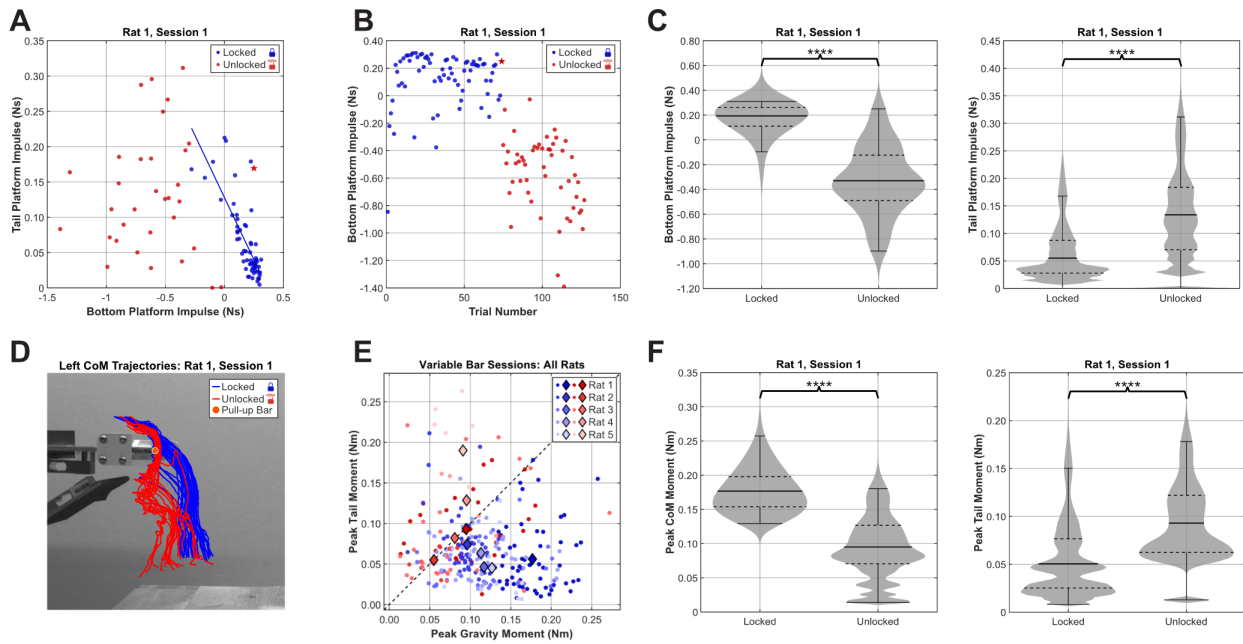


Fig. 4. Rats rapidly adapt their climbing strategy when forelimb torque is eliminated by unlocking the pull-up bar. **A.** Bottom platform impulse and tail platform impulse for the locked to unlocked bar session from Rat 1, showing a significant negative correlation during locked bar trials (blue, $n = 72$) but no significant correlation during unlocked bar trials (red, $n = 53$). The first unlocked trial is star shaped. **B.** Bottom platform impulse across sequential trials, illustrating the abrupt change immediately after transitioning from locked (blue) to unlocked (red) conditions. The first unlocked trial (red star) shows higher impulse than subsequent unlocked trials, indicating rapid adaptation after initial exposure. **C.** Distributions of bottom platform impulse (left) and tail platform impulse (right) for Rat 1. Bottom platform impulse show a significant decrease from locked (0.193 ± 0.091 Ns, $n = 58$) to unlocked (-0.330 ± 0.276 Ns, $n = 33$) conditions (Wilcoxon rank-sum test, $p < 0.001$, marked with asterisks). Tail platform impulse show a significant increase from locked (0.055 ± 0.040 Ns) to unlocked (0.134 ± 0.085 Ns) conditions (Wilcoxon rank-sum test, $p < .001$, marked with asterisks). **D.** Center-of-mass trajectories for Rat 1 during climbing of the left ledge in locked (blue) and unlocked (red) conditions. The position along the pull-up bar about which moments were taken is highlighted in orange. **E.** Relationship between peak gravity moment and peak tail moment across all rats ($n=5$) in both locked (blue) and unlocked (red) conditions. Diamond markers represent means for each condition for each rat. **F.** Distributions of peak center-of-mass moments (left) and peak tail moments (right) for Rat 1. Center-of-mass moments show a significant decrease from locked (0.177 ± 0.031 Nm, $n = 58$) to unlocked (0.095 ± 0.045 Nm, $n = 30$) conditions (Wilcoxon rank-sum test, $p < .001$, marked with asterisks). Tail moments show a significant increase from locked (0.050 ± 0.033 Nm, $n = 58$) to unlocked (0.093 ± 0.040 Nm, $n = 30$) conditions (Wilcoxon rank-sum test, $p < .001$, marked with asterisks).

from the jumping and gravitational impulse from Eq. (2) is too low, tail usage becomes necessary to supplement the angular impulse and prevent backward rotation under the bar due to gravity, thus rationalizing—in a causal manner—the inverse relationship between initial vertical impulse and subsequent tail use.

Depth Adaptation Strategy

Our finding that rats maintained consistent bottom platform impulse while significantly increasing tail usage at greater depths reveals an intriguing strategy preference. This adaptation pattern suggests that rats prioritize reliability over potentially more efficient but riskier approaches. While rats could theoretically increase their initial jumping impulse to compensate for greater depths, this would require the ability to judge the distance to the ledge with great precision, which is an ability that rats possess.

Despite rats having poor visual acuity—more than 20 times worse than humans (Artal et al., 1998)—they possess multiple sensory mechanisms for accurately perceiving spatial distances. Visual depth perception can be achieved through head bobbing and motion parallax (Legg and Lambert, 1990), as demonstrated in mice with monocular vision that compensate for reduced binocular depth cues by increasing head

bobbing behaviors while maintaining accurate jump distance adjustments (Parker et al., 2022). Additionally, rats can utilize tactile sensing through whisker contact to estimate distances, with whisker-based strategies enabling accurate gap distance estimation even when blinded (Hutson and Masterton, 1986). Proprioceptive feedback during forelimb extension toward the pull-up bar provides another reliable source of depth information. Given the numerous trials performed by each animal during both shallow and deep sessions, it is highly unlikely that depth differences went undetected through these combined sensory modalities. The fact that animals maintained consistent bottom platform impulse across depths indicates that depth perception was not the limiting factor in their climbing strategy. Rather, our results suggest that they strategically chose not to pre-calibrate their initial vertical leaping impulse. Instead, they employed a reliable initial impulse followed by adaptive tail-based corrections during the climbing phase.

It is also possible that keeping a consistent bottom platform impulse with increased tail usage suggests that rats separate the climbing task into distinct phases with different control strategies in a sequential composition (Burridge et al., 1999): an initial ballistic phase with relatively fixed parameters, followed by an adaptive correction phase where the tail provides fine-tuned adjustments. Such a strategy hypothetically allows

the rats to maintain reliable performance despite their visual limitations while effectively adapting to varying environmental challenges.

The outlier rat (4) demonstrated a notably different strategy, significantly decreasing bottom platform impulse while increasing tail usage in deeper conditions. This rat was observed to be generally less comfortable with the intended climbing method and more likely to adopt alternative approaches. This individual variation suggests that while the general strategy of tail-assisted climbing is consistent across animals, individual preferences, physical capabilities, or prior experiences can lead to different approaches to balancing risks and demands. Such variation may be attributed to the Minimum Intervention Principle—the motor system’s tendency to correct deviations only when they interfere with task success while allowing variability in task-irrelevant dimensions (Todorov and Jordan, 2002). Also, minute differences in training experiences could lead to persistent differences in preferred movement strategies. This has been demonstrated in other rodents in the context of tail usage, as untrained laboratory mice with intact tails often perform on par with trained mice without tails in balance tasks (Buck et al., 1925; Siegel, 1970). Rat 4’s preference for a more quasi-static climbing mode with lower bottom platform impulse and higher tail platform impulse likely represents a more conservative strategy that prioritizes stability at the expense of efficiency, similar to the climbing methods employed by rats in the unlocked bar sessions.

Rapid Adaptation to Mechanical Changes

Perhaps the most striking finding was the rats’ immediate adaptation to the unlocked bar condition. After just a single near-failure, rats significantly altered their strategy, decreasing bottom platform impulse and increasing tail platform impulse. This one-shot learning demonstrates remarkable sensorimotor intelligence and adaptability. The transition from parabolic center-of-mass trajectories in the locked condition to the characteristic “swing under then over” pattern in the unlocked condition reveals a fundamental shift in biomechanical strategy. Without the ability to generate moments at the forelimbs, rats categorically altered their approach, essentially solving a new motor problem on the fly.

The observed transition to a more quasi-static climbing mode in the unlocked bar condition suggests that rats prioritize stability and safety over energy efficiency when faced with challenging mechanical conditions. This parallels observations in other climbing animals, such as snakes that adopt energetically costly but mechanically stable patterns when navigating tree branches (Byrnes and Jayne, 2014). Beyond these stability adaptations, the rats also demonstrated impressive learning capabilities seen in other animals. Notably, the rats’ rapid motor learning resembles that of squirrels, which quickly modify their impulse generation upon repeated leaps from unfamiliar, compliant beams, improving landing accuracy over just five trials (Hunt et al., 2021). This remarkable capacity for rapid adaptation to environmental changes demonstrates how crucial behavioral plasticity is for rodent survival across varied and unpredictable terrains.

Our findings may also be interpreted through the lens of optimal control theory. The observed behavioral shift under unlocked bar conditions—from ballistic to quasi-static climbing with reduced initial impulse and increased tail usage—suggests that rats adapted not merely to compensate

for mechanical constraints, but in response to increased environmental uncertainty. This aligns with motor control frameworks proposed by Wolpert and colleagues (Wolpert et al., 1995), where the central nervous system integrates sensory feedback and internal predictions to minimize expected costs under uncertainty. An unstable support surface (the freely spinning bar) increases outcome variability, potentially favoring more conservative strategies with lower kinetic energy and greater corrective control authority through tail modulation. While we did not explicitly model this as a Bayesian optimization problem, the rapid strategy switching and consistent preference for controlled movements under uncertain conditions are consistent with adaptive motor planning that dynamically reweights movement strategies based on environmental feedback.

To understand how these adaptive strategies were mechanically implemented, we next examine the moments acting about the pull-up bar and how they were modulated in response to bar condition. In the locked bar case, rats produced peak tail moments that were lower than peak gravitation moments. Presumably, this is due in part to the fact that the animals can produce forelimb generated moments on the pull-up bar, and also because the animals would use a more ballistic exit from the bottom platform. We saw the animals modulate two variables in equation 3 to climb onto the ledge in the unlocked bar case. First, the animals increased F_t by directly increasing the forces generated by their tails on the tail platform. Second, the animals brought their center of mass closer to the bar, reducing L_g (the gravitational moment arm) and subsequently making it easier to produce compensatory tail-generated moments. All animals used one or more of these strategies, producing a control strategy for getting on top of the ledge such that, on average, $F_t L_t \geq mg L_g$ (see Figure 4).

General Themes and Broader Impact

These findings collectively enhance our understanding of several important aspects of animal locomotion and motor control. First, they demonstrate sophisticated motor control strategies that integrate information about initial conditions, environmental challenges, and mechanical constraints to produce adaptive behaviors. The predictable relationship between initial conditions and tail usage suggests rats possess internal models of task dynamics that allow them to anticipate necessary compensations.

Second, our results highlight remarkable task-level adaptation capabilities. Rats not only fine-tune parameters within a strategy (modulating tail force based on initial impulse) but can also rapidly switch between fundamentally different strategies when conditions change (as seen in the unlocked bar adaptation). This multi-level adaptation enables robust performance across varying conditions.

Third, these findings expand our understanding of tail function in climbing animals. Rather than serving merely as a passive counterbalance, the rat’s tail functions as an actively controlled appendage that generates substantial moments and contributes meaningfully to complex maneuvers, building on previous findings that demonstrate the similar dynamical tail during locomotion (Jusufi et al., 2008; Siddall et al., 2021).

These findings have potential applications in robotics, particularly for climbing robots that must navigate complex vertical environments. The stabilizing function of tails has already been incorporated into robotic systems (Chang-Siu et al., 2011; Spenko et al., 2008), but our findings suggest more

sophisticated control strategies based on sequential composition principles (Burridge et al., 1999).

In the context of sequential composition, funnels are regions of a system’s state space within which a particular feedback controller can reliably drive the system toward a goal. Each funnel represents the domain of attraction for a local controller—meaning that if the system’s state enters this funnel, the controller will guide it to a target state or behavior (a goal). If system trajectories always descend this funnel, the system is stable under that controller. However, because many tasks, such as climbing, involve regions where no single controller suffices to guarantee success across all initial conditions, multiple funnels are needed. These funnels can be sequentially composed, meaning the goal of one funnel lies within the domain of attraction of another. This allows a system to move through a series of stabilized subgoals—each governed by a different controller—until it reaches the final task goal.

Based on our observations, rats may employ a sequence of distinct control “funnels” to achieve successful climbing: the first funnel spans from when the hindlimbs leave the bottom platform until the tail connects with the tail platform, the second funnel extends from tail contact to when the center of mass positions over the ledge (with stable positioning atop the ledge being the goal state), and the third funnel is the locomotor gait that takes the rat to its ultimate food reward at the end of the ledge platform. Each funnel represents a distinct controller with different dynamics and constraints. Notably, when mechanical conditions changed in the unlocked bar condition, rats fundamentally altered these controllers—switching from a momentum-based approach to a quasi-static strategy where $F_t L_t \geq mg L_g$ became the governing relationship. Implementing similar condition-dependent switching between control funnels in robots could enhance their ability to navigate challenging vertical terrains. By dynamically modulating appendage forces based on mechanical constraints and detected instabilities, climbing robots could achieve greater robustness when encountering unexpected environmental changes.

Importantly, the linkages between these funnels may critically shape the success of the overall maneuver. For instance, a cautious takeoff with reduced impulse could position the animal within a broader or more stable region of the next funnel’s domain, making tail engagement and subsequent stabilization more likely. Conversely, an aggressive or mistimed jump could deposit the animal outside the next controller’s basin of attraction, requiring corrective action to reach the goal state or leading to failure.

Rats are not only capable of sophisticated locomotor behaviors, as demonstrated in this study, but are also champion model organisms in neuroscience research. This unique intersection makes them ideal subjects for exploring neural components of complex motor tasks. For example, Green et al. (Green et al., 2022) recently characterized the patterns of hippocampal activity in rats as they perform a horizontal jumping task. The behavioral paradigm in this study also has implications for understanding neural control and motor planning. The rats’ ability to rapidly adapt climbing strategies to mechanical changes suggests involvement of higher-level sensorimotor integration that coordinates with motor control systems. This climbing behavior necessitates interaction between multiple neural systems, particularly those involved in proprioception, spatial representations, and motor planning. Future studies might explore this neural basis by recording from sensorimotor regions during climbing tasks to

better understand how these neural networks facilitate the adaptive climbing behaviors we observed.

Despite the ubiquity of *R. norvegicus* in both research and urban environments, relatively little is known about how these animals use their tails during natural climbing behaviors, through a biomechanical lens. While some comparative work has explored tail length and arboreal performance across rodent species—such as ship rats having longer tails that enhance tree-climbing ability (Foster et al., 2011), or correlations between tail morphology and habitat in deer mice (Hager and Hoekstra, 2021)—analogous studies in laboratory rats are scarce. Without a clearer understanding of how rats like *R. norvegicus* move in environments similar to those encountered in the wild, it remains challenging to fully contextualize these findings within broader patterns of rat tail evolution. Future work integrating biomechanics, comparative morphology, and behavioral ecology could help clarify the role of the tail in supporting locomotor versatility in this widespread species. Notably, this study used only male Long-Evans rats—a strain of *R. norvegicus* commonly used in laboratory environments. This is a limitation as potential sex and strain differences during this task were not explored. Sex-specific variations (such as body mass distribution and risk assessment behaviors) could influence climbing strategies, and thus affect tail usage patterns. Additionally, strain differences in physical capabilities and behavioral tendencies might further affect these patterns. Future studies incorporating female rats and different strains would enhance the generalizability of our findings and potentially reveal sex-specific or strain-specific adaptations in tail-assisted climbing behaviors.

It is also important to note other caveats and shortcomings of the study. While our use of LMMs allowed us to account for hierarchical structure in the dataset and isolate the effects of key experimental factors, it is important to recognize that the underlying biomechanics of climbing are inherently nonlinear. The forces, moments, and state transitions involved in tail climbing behavior involve complex interactions between body segments, varying moment arms, and time-dependent motor outputs. However, LMMs provided a statistically tractable first-order approximation of these relationships, enabling us to identify consistent effects across animals and sessions while accounting for between-subject variability. Also, the scope of the template model (Eq. 3) is limited, as it does not incorporate any terms related to body or tail bending or shape change. Future work could leverage more complex simulation environments, such as MuJoCo (Todorov et al., 2012), to incorporate these biomechanical details and produce a more biologically grounded model. However, we believe the value of the simplified model is not lost, as it provided a useful framework for generating testable hypotheses that guided the design of this study.

We recognize that direct neuromechanical measurements—such as neuronal or EMG recordings—would be valuable to support our conclusion that rats actively controlled their tails during this climbing task. However, our conclusion is nevertheless supported by behavioral evidence, including kinematics and force measurements. While it is impossible to confirm that active tail use was significant during every trial, we observed many trials in which the tail clearly produced prolonged, forceful contact with the platforms of the experimental rig that are not easily explained by passive motion alone. See, for example Supplemental Video S4 shows a trial in which the tail pressed against the tail platform at an elevated angle of 60 degrees; this clearly required muscle activation

to both overcome gravity and apply a significant, sustained normal force. In Supplemental Video S5, the tail applied a sustained downward force on the bottom platform that far exceeded the expected passive weight of the tail segment, and maintained that force for half a second—a duration and magnitude inconsistent with purely passive dynamics. These behaviors, combined with the increase in tail forces during mechanically challenging conditions (such as unlocked bar trials), suggest that the tail is not merely reacting to motion of the body but is being actively deployed. Lastly, the fact that our model predicted these qualitative features for how tail forces should be modulated as a function of behavior provides further evidence that the tail is actively controlled.

While this study focused on stereotyped climbing behaviors, we also observed interesting variations and novel solutions that did not occur with sufficient frequency for statistical analysis. These behaviors included squeezing between the pull-up bar and the ledge, climbing around the side of the ledge to avoid the unlocked pull-up bar, and arresting a fall from the bottom platform by pushing off the tail platform (Supplemental Videos S6, S7, and S8, respectively). These observations highlight the remarkable behavioral flexibility and problem-solving capabilities of rats and suggest directions for future investigations.

In conclusion, our study reveals that the rat's tail is an adaptive, actively controlled appendage that contributes significantly to climbing performance through dynamic force application. Rats demonstrate remarkable adaptability in their tail usage, modifying their strategies based on both initial conditions and changing task demands. These findings enhance our understanding of how auxiliary appendages contribute to complex motor tasks and may inspire novel approaches in fields ranging from comparative biomechanics to robotics design.

Competing interests

No competing interest is declared.

Author contributions statement

Conceptualization: BMW, NJC, and SGL. Methodology: BMW and NJC. Investigation: BMW and NCG. Data curation: BMW and NCG. Formal analysis: BMW. Software: BMW, NCG, and SGL. Visualization: BMW. Writing – original draft: BMW, with input from NJC.

Acknowledgments

We thank the American Association for Anatomy, Company of Biologists, and the SICB Division of Comparative Biomechanics for sponsoring and funding this symposium. This work was supported by Army Research Office Multi-disciplinary University Research Initiative (MURI) Program Award W911NF1810327 and National Institutes of Health (NIH) Award R01 NS102537 from the NINDS. We thank Dr. James J. Knierim for his invaluable mentorship in rat handling, training, behavior, and neuroscience. We are grateful to Murtaza Hathiari for his contributions to the early stages of this project.

Data availability

The data for the analysis and results described in this paper will be made available via the Johns Hopkins Research Data Repository at <https://doi.org/10.7281/T1H0NHZE> upon final acceptance.

References

- P. Artal, P. H. de Tejada, C. M. Tedó, and D. G. Green. Retinal image quality in the rodent eye. *Visual Neuroscience*, 15(4): 597–605, 1998.
- G. A. Bartholomew and H. H. Caswell. Locomotion in kangaroo rats and its adaptive significance. *Journal of Mammalogy*, 32(2):155–169, 1951.
- C. Buck, N. Tolman, and W. Tolman. The tail as a balancing organ in mice. *Journal of Mammalogy*, 6(4):267–271, 1925.
- J. Buckley, N. Chikere, and Y. Ozkan-Aydin. The effect of tail stiffness on a sprawling quadruped locomotion. *Frontiers in Robotics and AI*, 10:1198749, 2023.
- R. R. Burridge, A. A. Rizzi, and D. E. Koditschek. Sequential composition of dynamically dexterous robot behaviors. *The International Journal of Robotics Research*, 18(6):534–555, 1999.
- G. Byrnes and B. C. Jayne. Gripping during climbing of arboreal snakes may be safe but not economical. *Biology Letters*, 10(8):20140434, 2014.
- E. Chang-Siu, T. Libby, M. Tomizuka, and R. J. Full. A lizard-inspired active tail enables rapid maneuvers and dynamic stabilization in a terrestrial robot. In *IEEE/RSJ International Conference on Intelligent Robots and Systems*, pages 1887–1894. IEEE, 2011.
- S. Foster, C. King, B. Patty, and S. Miller. Tree-climbing capabilities of norway and ship rats. *New Zealand Journal of Zoology*, 38(4):285–296, 2011.
- R. J. Full and D. E. Koditschek. Templates and anchors: neuromechanical hypotheses of legged locomotion on land. *Journal of Experimental Biology*, 202(23):3325–3332, 1999.
- L. Green, D. Tingley, J. Rinzel, and G. Buzsáki. Action-driven remapping of hippocampal neuronal populations in jumping rats. *Proceedings of the National Academy of Sciences*, 119(26):e2122141119, 2022.
- E. R. Hager and H. E. Hoekstra. Tail length evolution in deer mice: linking morphology, behavior, and function. *Integrative and Comparative Biology*, 61(2):385–397, 2021.
- G. C. Hickman. The mammalian tail: a review of functions. *Mammal Review*, 9(4):143–157, 1979.
- N. H. Hunt, J. Jinn, L. F. Jacobs, and R. J. Full. Acrobatic squirrels learn to leap and land on tree branches without falling. *Science*, 373(6555):697–700, 2021.
- K. Hutson and R. Masterton. The sensory contribution of a single vibrissa's cortical barrel. *Journal of Neurophysiology*, 56(4):1196–1223, 1986.
- A. Jusufi, D. I. Goldman, S. Revzen, and R. J. Full. Active tails enhance arboreal acrobatics in geckos. *Proceedings of the National Academy of Sciences*, 105(11):4215–4219, 2008.
- S. A. Lacava, N. Isilak, and M. Y. Uusisaari. The role of mouse tails in response to external and self-generated balance perturbations on the roll plane. *Journal of Experimental Biology*, 227(21), 2024.
- S. D. Lee, S. Wang, D. Kuang, E. K. Wang, J. K. Yim, N. H. Hunt, R. S. Fearing, H. S. Stuart, and R. J. Full. Free-ranging squirrels perform stable, above-branch landings by balancing using leg force and nonprehensile foot torque. *Journal of*

884 *Experimental Biology*, pages jeb-249934, 2025.

885 C. Legg and S. Lambert. Distance estimation in the hooded
 886 rat: experimental evidence for the role of motion cues.
 887 *Behavioural Brain Research*, 41(1):11–20, 1990.

888 T. Libby, T. Y. Moore, E. Chang-Siu, D. Li, D. J. Cohen,
 889 A. Jusufi, and R. J. Full. Tail-assisted pitch control in lizards,
 890 robots and dinosaurs. *Nature*, 481(7380):181–184, 2012.

891 I. J. Makowska and D. M. Weary. The importance of burrowing,
 892 climbing and standing upright for laboratory rats. *Royal
 893 Society Open Science*, 3(6):160136, 2016.

894 A. Mathis, P. Mamidanna, K. M. Cury, T. Abe, V. N. Murthy,
 895 M. W. Mathis, and M. Bethge. Deeplabcut: markerless pose
 896 estimation of user-defined body parts with deep learning.
 897 *Nature Neuroscience*, 21(9):1281–1289, 2018.

898 R. Å. Norberg. Treecreeper climbing; mechanics, energetics,
 899 and structural adaptations. *Ornis Scandinavica*, pages 191–
 900 209, 1986.

901 T. Notomi, N. Okimoto, Y. Okazaki, Y. Tanaka, T. Nakamura,
 902 and M. Suzuki. Effects of tower climbing exercise on bone
 903 mass, strength, and turnover in growing rats. *Journal of
 904 Bone and Mineral Research*, 16(1):166–174, 2001.

905 P. R. Parker, E. T. Abe, N. T. Beatie, E. S. Leonard, D. M.
 906 Martins, S. L. Sharp, D. G. Wyrick, L. Mazzucato, and
 907 C. M. Niell. Distance estimation from monocular cues in
 908 an ethological visuomotor task. *Elife*, 11:e74708, 2022.

909 M. J. Schwaner, G. A. Freymiller, R. W. Clark, and C. P.
 910 McGowan. How to stick the landing: kangaroo rats use their
 911 tails to reorient during evasive jumps away from predators.
 912 *Integrative and Comparative Biology*, 61(2):442–454, 2021.

913 S. Shield, R. Jericevich, A. Patel, and A. Jusufi. Tails,
 914 flails, and sails: how appendages improve terrestrial
 915 maneuverability by improving stability. *Integrative and
 916 Comparative Biology*, 61(2):506–520, 2021.

917 R. Siddall, G. Byrnes, R. J. Full, and A. Jusufi. Tails stabilize
 918 landing of gliding geckos crashing head-first into tree trunks.
 919 *Communications Biology*, 4(1):1020, 2021.

920 M. I. Siegel. The tail, locomotion and balance in mice.
 921 *American Journal of Physical Anthropology*, 33(1):101–102,
 922 1970.

923 M. J. Spenko, G. C. Haynes, J. Saunders, M. R. Cutkosky,
 924 A. A. Rizzi, R. J. Full, and D. E. Koditschek. Biologically
 925 inspired climbing with a hexapedal robot. *Journal of Field
 926 Robotics*, 25(4-5):223–242, 2008.

927 E. Todorov and M. I. Jordan. Optimal feedback control as a
 928 theory of motor coordination. *Nature Neuroscience*, 5(11):
 929 1226–1235, 2002.

930 E. Todorov, T. Erez, and Y. Tassa. Mujoco: A physics engine
 931 for model-based control. In *2012 IEEE/RSJ international
 932 conference on intelligent robots and systems*, pages 5026–
 933 5033. IEEE, 2012.

934 D. M. Wolpert, Z. Ghahramani, and M. I. Jordan. An internal
 935 model for sensorimotor integration. *Science*, 269(5232):1880–
 936 1882, 1995.